III. Conclusion

We have presented the characteristic impedance of the slab line with an anisotropic dielectric. The characteristic impedance has been obtained analytically by using transform methods. A simpler approximate formula which is useful for application has also been presented.

Acknowledgment

The authors would like to thank the reviewers for helpful suggestions, and T. Koizumi of Ibaraki College of Technology for helpful comments that have improved the readability of the paper.

References

[1] S Frankel, "Characteristic impedance of parallel wires in rectangular troughs," *Proc IRE*, vol. 30, pp. 182–190, Apr. 1942.

[2] W B. Wholey and W N. Eldred, "A new type of slotted line section," *Proc. IRE*, vol. 38, pp. 244–248, Mar. 1950.

[3] H. A. Wheeler, "The transmission-line properties of a round wire between parallel planes," *IRE Trans. Antennas Propagat.*, vol. AP-3, pp. 203–207, Oct. 1955.

[4] R M. Chisholm, "The characteristic impedance of trough and slab lines," *IRE Trans. Microwave Theory Tech.*, vol. MTT-4, pp. 166–172, July 1956.

[5] H. A. Wheeler, "Transmission-line properties of a round wire in a polygon shield," *IEEE Trans. Microwave Theory Tech.*, vol. MTT-27, pp 717–721, Aug. 1979.

[6] B T. Szentkuti, "Simple analysis of anisotropic microstrip lines by a transform method," *Electron. Lett.*, vol. 12, pp. 672–673, Dec. 1976.

[7] N. G Alexopoulos, S. Kerner, and C. M. Krowne, "Dispersionless coupled microstrip over fused silica-like anisotropic substrates," *Electron. Lett.*, vol. 12, pp. 579–580, Oct. 1976.

[8] N. G Alexopoulos and C. M. Krowne, "Characteristics of single and coupled microstrips on anisotropic substrates," *IEEE Trans. Microwave Theory Tech.*, vol. MTT-26, pp 387–393, June 1978.

[9] N. G. Alexopoulos and N. K. Uzunoglu, "An efficient computation of thick microstrip properties on anisotropic substrates," *J. Franklin Inst.*, vol. 306, pp. 9–22, July 1978.

[10] S Kusase and R. Terakado, "Mapping theory of two-dimensional anisotropic regions," *Proc. IEEE*, vol. 67, pp. 171–172, Jan. 1979

[11] A. G. d'Assuncao, A. J. Giarola, and D. A. Rogers, "Analysis of single and coupled striplines with anisotropic substrates," in *IEEE MTT-S Int. Microwave Symp. Dig.*, June 1981, pp. 83–85.

[12] H Shibata, S. Minakawa, and R. Terakado, "Analysis of the shielded-strip transmission line with an anisotropic medium," *IEEE Trans. Microwave Theory Tech.*, vol MTT-30, pp. 1264–1267, Aug. 1982.

[13] H. Shibata, S. Minakawa, and R. Terakado, "A numerical calculation of the capacitance for the rectangular coaxial line with offset inner conductor having an anisotropic dielectric," *IEEE Trans. Microwave Theory Tech.*, vol MTT-31, pp. 385–391, May 1983.

[14] M Horno, "Quasistatic characteristics of covered coupled microstrips on anisotropic substrates: Spectral and variational analysis," *IEEE Trans. Microwave Theory Tech.*, vol. MTT-30, pp. 1888–1892, Nov. 1982.

[15] T Kitazawa and Y. Hayashi, "Propagation characteristics of striplines with multilayered anisotropic media," *IEEE Trans. Microwave Theory Tech.*, vol. MTT-31, pp. 429–433, June 1983.

[16] S. K. Koul and B. Bhat, "Generalized analysis of microstrip-like transmission lines and coplaner strip with anisotropic substrates for MIC, electrooptic modulator, and SAW application," *IEEE Trans. Microwave Theory Tech.*, vol. MTT-31, pp 1051–1059, Dec. 1983.

[17] J. Fontanella, C. Andeen, and D. Schuele, "Low-frequency dielectric constants of α-quartz, sapphire, M_gF_2, and M_gO," *J. Appl. Phys.*, vol. 45, pp. 2852–2854, July 1974.

[18] C. M. Krowne, "Microstrip transmission lines on pyrolytic boron nitride," *Electron. Lett.*, vol. 12, pp. 642–643, Nov. 1976.

[19] K V. S. Rao and B. N. Das, "Stripline using an oval-shaped centre conductor between grounded planes," *Proc. Inst. Elec. Eng.*, vol 129, pt. H, pp. 366–368, Dec. 1982

[20] B N Das and K. V. S. Rao, "Analysis of an elliptical conducting rod between parallel ground planes by conformal mapping," *IEEE Trans. Microwave Theory Tech.*, vol: MTT-30, pp. 1079–1085, July 1982

[21] F Bowman, *Introduction to Elliptic Functions with Applications.* New York: Dover, 1961, pp. 22.

Edge-Guided Magnetostatic Mode in a Ridged-Type Waveguide

MORIYASU MIYAZAKI, KEN'ICHIRO YASHIRO, MEMBER, IEEE, AND SUMIO OHKAWA, SENIOR MEMBER, IEEE

***Abstract* — A ridged-type magnetostatic waveguide is analyzed using the boundary element method. A bias magnetic field is applied perpendicularly to the surface of an yttrium-iron-garnet (YIG) film grown on a gadlinium-gallium-garnet (GGG) substrate. The dispersion curves and the potential profiles obtained in this paper show that the mode has a strong nonreciprocal property and is a kind of edge-guided mode which propagates along either side of the ridge, depending upon the direction of the bias field and the direction of the wave propagation. In addition, the authors emphasize the fact that the boundary element method is useful for analysis of a complex structure in the field of magnetostatic wave (MSW) devices.**

I. Introduction

In a previous paper [1], the authors have already shown that the boundary element method (BEM) [2] is very effective and useful for the analysis of magnetostatic wave (MSW) problems. In the present paper, a ridged-type waveguide will be treated. Tanaka and Shimizu [3] obtained the dispersion relation for the same type of waveguide as discussed here, but the bias magnetic field was applied in the plane of the yttrium-iron-garnet (YIG) film and, therefore, the mode properties obtained there are quite different from those revealed here. Moreover, they used the equivalent-circuit method to get the results and, hence, did not show any potential profile.

For the purpose of application of MSW to microwave integrated circuits, it is desirable that a bias magnetic field be applied in the normal direction to the YIG film grown on the gadlinium-gallium-garnet (GGG) substrate. As is well known, however, only a magnetostatic volume wave (MSVW) can propagate in an infinite and homogenous YIG film.

Now, notice that the ridged structure has a side parallel or tilted to the bias field, and we might expect that the side or the wall of the ridge can support a kind of magnetostatic surface wave (MSSW). We may suggest that this type of guided wave stems from almost the same idea as guided MSW's in the plate of YIG magnetized nonuniformly [4]–[6]. Thus, it is very interesting to investigate the characteristics of the wave propagation along the ridged structure, and, besides, the authors would like to emphasize the fact that the BEM is very suitable for the analysis of a complex structure like this one.

II. BEM Formulation

The BEM approach for MSW propagation problems is described briefly below. A waveguide to be considered is shown in Fig. 1. A cross section of a waveguide may be arbitrary, but an internal dc magnetic field is supposed to be uniform for the sake of mathematical simplicity. Under a quasistatic approximation,

Manuscript received May 16, 1984; revised January 4, 1985 This work was supported in part by Grant-in-Aid for Scientific Research from the Ministry of Education of Japan.

M Miyazaki was with the Department of Electronic Engineering, Chiba University. He is now with Mitsubishi Electric Corp., Kamakura, Japan.

K Yashiro and S. Ohkawa are with the Department of Electronic Engineering, Chiba University, 1-33, Yayoi-cho, Chiba 260, Japan.

0018-9480/85/0500-0421$01.00 ©1985 IEEE

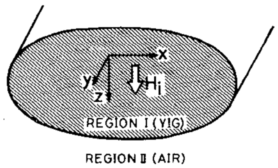

Fig. 1. Cross section of a waveguide for the magnetostatic wave. H_i is a bias magnetic field.

the Maxwell's equations yield to $\nabla \times \boldsymbol{h} = 0$ and $\nabla \cdot \boldsymbol{b} = 0$. Hence, the MSW's are described by the potential ϕ, from which $\boldsymbol{h} = \nabla\phi$. The basic equations are given as

$$\mu\frac{\partial^2\phi}{\partial x^2} + \frac{\partial^2\phi}{\partial z^2} - \mu\beta^2\phi = 0 \qquad \text{for YIG region} \tag{1}$$

$$\frac{\partial^2\phi}{\partial x^2} + \frac{\partial^2\phi}{\partial z^2} - \beta^2\phi = 0 \qquad \text{for air region} \tag{2}$$

with a variation factor $\exp[j(\omega t - \beta y)]$ understood, where μ is a diagonal component of the tensor permeability of YIG.

Applying the BEM to each of (1) and (2), we obtain the following matrix equations [1]:

$$H_{\mathrm{I}}\boldsymbol{\phi}_{\mathrm{I}} = \mathbf{G}_{\mathrm{I}}\boldsymbol{q}_{\mathrm{I}} \tag{3}$$

$$H_{\mathrm{II}}\boldsymbol{\phi}_{\mathrm{II}} = G_{\mathrm{II}}\mathbf{q}_{\mathrm{II}} \tag{4}$$

where $\boldsymbol{\phi}_{\mathrm{I,II}}$ and $\boldsymbol{q}_{\mathrm{I,II}}$ vectors are the values of the magnetic potentials and the normal components of the magnetic flux density at the boundary nodes, respectively, and the elements of the matrices $H_{\mathrm{I,II}}$ and $G_{\mathrm{I,II}}$ are calculated by using a fundamental solution with material constants of the medium in each region as follows [1]:

$$h_{ij} = \int_{\Gamma_{j-1}} \psi_2 \mathbf{q}_i^* \, d\Gamma + \int_{\Gamma_j} \psi_1 q_i^* \, d\Gamma + c_i\delta_{ij} \tag{5}$$

$$g_{ij} = \int_{\Gamma_{j-1}} \psi_2 \phi_i^* \, d\Gamma + \int_{\Gamma_j} \psi_1 \phi_i^* \, d\Gamma \tag{6}$$

$$\phi_i^* = \frac{1}{2\pi\sqrt{\mu}} K_0\left(\beta\sqrt{(x - x_i)^2 + \mu(z - z_i)^2}\right) \tag{7}$$

$$q_i^* = \left(\mu\frac{\partial\phi_i^*}{\partial x} - \kappa\beta\phi_i^*\right)n_x + \frac{\partial\phi_i^*}{\partial z}n_z \tag{8}$$

$$c_i = 1 - \frac{1}{2\pi}\left\{\tan^{-1}\left(\sqrt{\mu}\tan\theta_2\right) - \tan^{-1}\left(\sqrt{\mu}\tan\theta_1\right)\right\} \tag{9}$$

where (x, z) and (x_i, z_i) are coordinates of the source and observation point, respectively, δ_{ij} is the Kronecker delta, K_0 is the modified Bessel function of zero order, κ is an off-diagonal component of tensor permeability, n_x and n_z are x and z components of the normal unit vector, and θ_1 and θ_2 are the angles between the x-axis and the tangent to the boundary. ψ_1 and ψ_2 are the interpolation functions defined by

$$\psi_1 = (1 - \xi)/2$$
$$\psi_2 = (1 + \xi)/2, \qquad -1 \leqq \xi \leqq 1 \tag{10}$$

for the integral along the boundary element Γ_j, which does not include the observation point, and

$$\psi_1 = 1 - \xi$$
$$\psi_2 = \xi, \qquad 0 \leqq \xi \leqq 1 \tag{11}$$

for the integral along Γ_j, which includes the observation point. The integrals given in (5) and (6) are evaluated by the Gaussian quadrature numerical integration method.

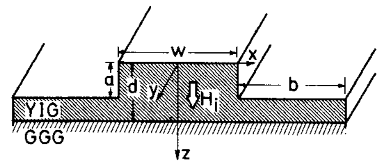

Fig. 2. Cross section of ridged-type waveguide.

The boundary conditions require the continuity of the tangential magnetic field and the normal flux density across a boundary contour. The tangential magnetic field is decomposed into the longitudinal component h_y and the transverse component h_t. Since the magnetic field can be computed from the gradient of the potential, h_y is equal to $-j\beta\phi$. h_t is also continuous across the contour if ϕ just inside the contour has the same variation along the contour as ϕ does just outside. Hence, (3) and (4) are combined with each other through boundary conditions, i.e., $\boldsymbol{\phi}_{\mathrm{I}} = \boldsymbol{\phi}_{\mathrm{II}}$ and $\boldsymbol{q}_{\mathrm{I}} = -\boldsymbol{q}_{\mathrm{II}}$, where the minus sign before $\boldsymbol{q}_{\mathrm{II}}$ indicates that the unit vector normal to the air region points to the opposite direction of the normal unit vector to the YIG region. Then, the following linear homogeneous system is obtained:

$$\begin{pmatrix} H_{\mathrm{I}} & -G_{\mathrm{I}} \\ H_{\mathrm{II}} & G_{\mathrm{II}} \end{pmatrix}\begin{pmatrix} \boldsymbol{\phi}_{\mathrm{I}} \\ \boldsymbol{q}_{\mathrm{I}} \end{pmatrix} = 0. \tag{12}$$

The determinant of the coefficient matrix in the above equation must be zero in order that a nontrivial solution exists, therefore

$$\begin{vmatrix} H_{\mathrm{I}} & -G_{\mathrm{I}} \\ H_{\mathrm{II}} & G_{\mathrm{II}} \end{vmatrix} = 0. \tag{13}$$

Successive values of the parameter β are tried until (13) is satisfied within some predetermined accuracy. It is easy to extend the BEM to analyze similar problems in which we consider more than two media.

III. Dispersion Relation and Potential Distribution

Consider a topographical structure, as illustrated in Fig. 2, as a practical MSW waveguide. A dc-bias magnetic field is applied along the z-axis, and we shall confine our discussions within the frequency range of the MSSW. In order to obtain a dispersion relation and a potential distribution, the computations were carried out by setting 77 nodes on the boundary for the BEM procedure. The other numerical values used there are given as follows:

bias field $H_i = 500$ Oe,
saturation magnetization $4\pi M_s = 1760$ G,
gyromagnetic ratio $\gamma = 2.8$ MHz/Oe,
width of the ridge $w = 100$ μm,
thickness of the ridge $d = 20$ μm,
ratio of height to thickness $(a/d) = 1.0, 0.9, 0.7, 0.5$.

Concerning the length of skirt b, it was taken so long as the potential was considered to decay out at the edge of YIG away from the ridge.

Fig. 3 shows the dispersion relation. We can see the curves become closer to those in the case of $a/d = 1$, which means the structure is reduced to a simple slab, as the parameter a/d approaches to unity. From another point of view, we can say that a wavenumber increases as a/d decreases. In the region of a smaller wavenumber, the side or wall of the ridge likely plays a less effective role; thus, it seems that the dispersion curves get nearer at the lower limit of the MSSW spectrum. The magneto-

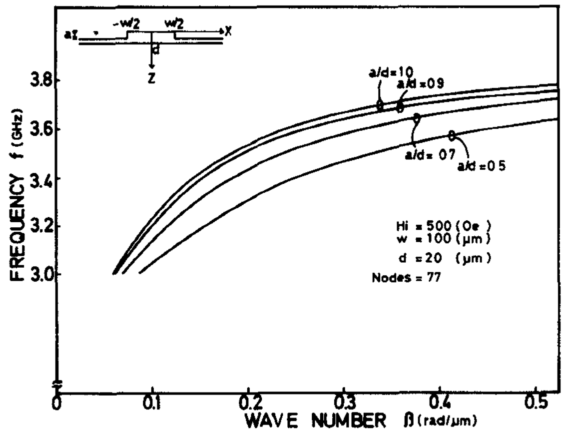

Fig 3 Dispersion of the magnetostatic wave propagating in the topographic ridge guide.

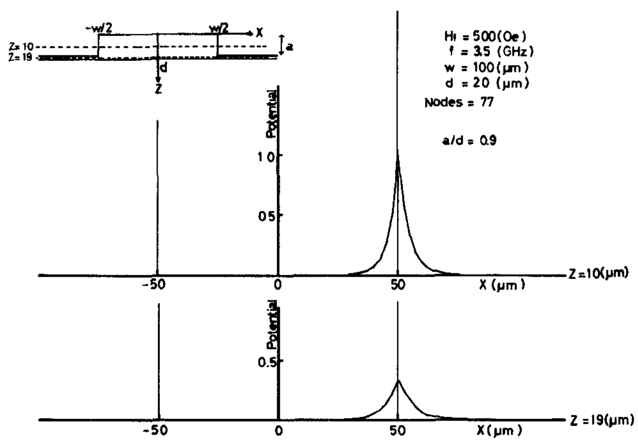

Fig. 4. Magnetic potential versus distance along the x-axis. Ratio a/d is equal to 0.9.

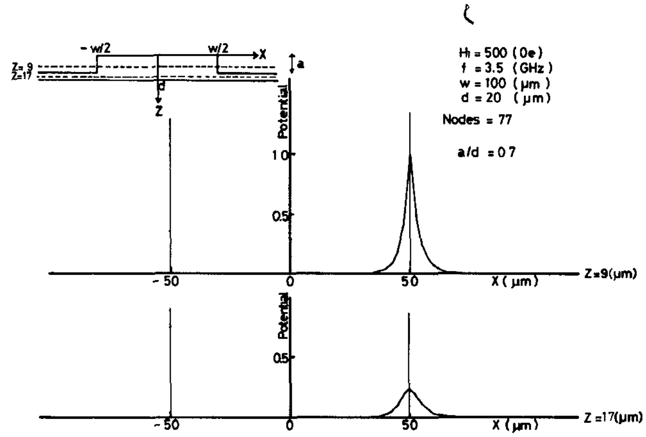

Fig. 5. Magnetic potential versus distance along the x-axis. Ratio a/d is equal to 0.7.

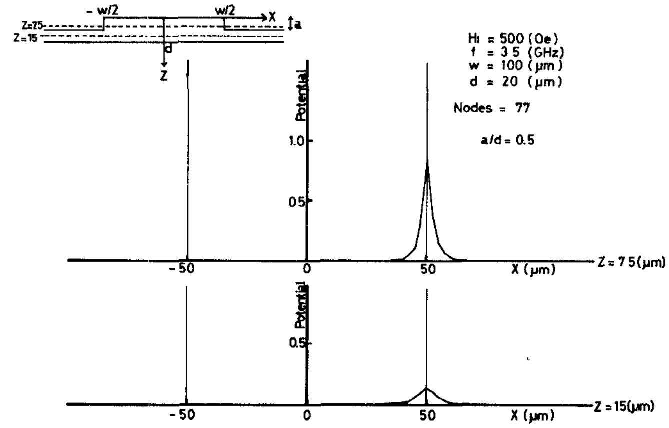

Fig. 6. Magnetic potential versus distance along the x-axis. Ratio a/d is equal to 0.5.

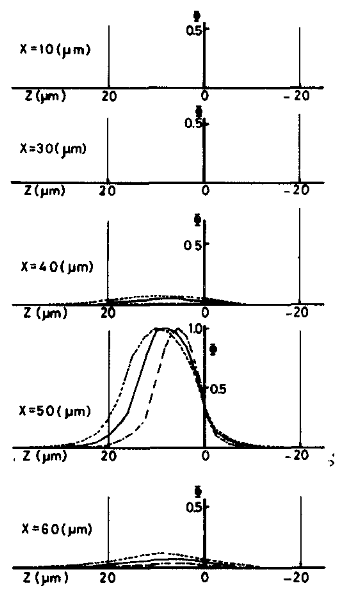

Fig. 7 Magnetic potential versus distance along the z-axis: ----- $a/d = 0.9$, —— $a/d = 0.7$, -·-·- $a/d = 0.5$.

static wave may be expected to have a sinusoidal variation along the x-axis below the surface-wave range, as is known in a width mode [7]. Unfortunately, the BEM cannot be applied directly to analysis in the volume-wave range.

In order to realize the mode characteristic, let's see the potential profile. Several patterns are shown in Figs. 4–7. All potential profiles are obtained along the dotted lines in these figures, keeping the frequency at 3.5 GHz. As is seen from these curves, the most important and characteristic feature is that the mode obtained here is nonreciprocal and a kind of so-called edge-guided mode along the wall of the ridge. The energy concentration at the edge is conspicuous, and, for instance, the potential decays below 10 percent of its peak somewhere away from the edge by only 0.2 wavelengths. Also, it is noteworthy that the energy concentration increases remarkably as the ratio a/d decreases. To sum up, the mode has a strong nonreciprocity and well-guided property. Fig. 7 shows how the potential varies along the z-axis, that is, in the direction of the depth of the ridge. We see that each peak corresponding to the respective a/d ratio is reasonably located at around the center of the wall.

IV. Conclusions

In the present paper, the authors proposed a ridged-type waveguide for MSW's which was supposed to be practical from the following standpoints. Firstly, a bias magnetic field is applied in the direction normal to the surface of the substrate. Secondly, it is not difficult to fabricate the geometry by chemical etching.

The BEM was used for computations of the dispersion relations and the potential distributions. In conclusion, there exists a nonreciprocal mode which propagates along either one side of the ridge or another, depending upon the direction of the bias field and the direction of wave propagation. For instance, we have an edge-guided mode with wavelength = 19 μm, phase velocity = 6.7

$\times 10^4$ m/s, and group velocity $= 8.4 \times 10^3$ m/s at frequency = 3.5 GHz for the case of $d = 20$ μm, $a = 10$ μm, and $w = 100$ μm. The potential in this case decays below 10 percent of its peak when it is away from the wall by 0.2 wavelength. This represents the extent of the energy concentration and at the same time the extent of nonreciprocity of the waveguide. The knowledge about the mode treated here immediately gives us an idea that the proposed structure is effectively available for isolators, circulators, and so forth in a way similar to the edge-guided mode in a ferrite loaded stripline [8].

As mentioned in Section I, the authors would like to have made clear not only that the proposed waveguide is promising in the field of MSW devices, but also that the BEM is useful for the analysis of structures for which analytical solutions are not obtained simply or easily. It may be worthwhile to point out that the computer program developed by the authors makes complex computations possible in such cases as a disc and periodically corrugated waveguides.

References

[1] K. Yashiro, M. Miyazaki, and S Ohkawa, "Boundary element method approach to magnetostatic wave problems," *IEEE Trans. Microwave Theory Tech.*, vol. MTT-33, pp. 248–253, Mar. 1985.

[2] C. A. Brebbia, *The Boundary Element Method for Engineers*. London: Pentech Press, 1978.

[3] H. Tanaka and H. Shimizu, "On the waveguide for magnetostatic surface waves," *Trans. IECE Japan*, vol. J63-B, pp 651–653, June 1980.

[4] F. R. Morgenthaler, "Bound magnetostatic waves controlled by field gradients in YIG single crystals and epitaxial films," *IEEE Trans Magn.*, vol. MAG-14, pp. 806–810, Sept. 1978.

[5] M. Tsutsumi, Y. Masaoka, T. Ohira, and N. Kumagai, "A new technique for magnetostatic wave delay lines," *IEEE Trans. Microwave Theory Tech.*, vol. MTT-29, pp. 583–589, June 1981

[6] K. Yahiro and S. Ohkawa, "Guided magnetostatic waves of the YIG plate magnetized nonuniformly," *IEEE Trans. Microwave Theory Tech.*, vol. MTT-29, pp. 745–747, July 1981.

[7] T. W. O'Keeffe and R. W. Patterson, "Magnetostatic surface-wave propagation in finite samples," *J. Appl. Phys.*, vol. 49, pp. 4886–4895, Sept. 1978

[8] K. Araki, T. Koyama, and Y. Naito, "Reflection problems in a ferrite stripline," *IEEE Trans Microwave Theory Tech.*, vol. MTT-24, pp. 491–498, Aug. 1976.

A New Recurrence Method for Determining the Green's Function of Planar Structures with Arbitrary Anisotropic Layers

RICARDO MARQUÉS, MANUEL HORNO, MEMBER IEEE, AND FRANCISCO MEDINA

***Abstract*—A method to determine the Green's functions in the spectral domain is developed. It is suitable for solving the matrix Green's function numerically for an arbitrary anisotropic N-layered dielectric structure. The method is suitable for computation of the characteristic parameters of MIC lines having anisotropic multilayered substrates or superstrates. As an application, the phase velocities of single and coupled microstrips, with a constant gradient of anisotropy along the normal to the interfaces, have been calculated.**

Manuscript received March 12, 1984; revised January 4, 1985.

The authors are with the Departamento de Electricidad y Electrónica, Facultad de Física, Universidad de Sevilla, Seville, Spain.

I. Introduction

During the last several years, the conventional planar structures embedded in anisotropic dielectrics—single [1]–[4], coupled [5]–[8], covered [9]–[11], shielded microstripline [12], [13], slotline [14], and coplanar waveguide [15]—have been analyzed extensively.

The most commonly used anisotropic substrates, such as sapphire and boron–nitride, or some glass- and ceramic-filled polymeric materials, e.g. Duroid and Epsilam, have well-known advantages over the isotropic substrates used largely in microwave integrated circuits. The introduction of anisotropic substrates having tilted principal axes has recently made it possible to manipulate some characteristic parameters of the structure in a range depending on the substrate anisotropy. For instance, it has been shown that the phase velocities can be equalized by varying the tilting angle in the coupled microstriplines [7].

The propagation characteristics study of such structures has been made using various procedures. Nevertheless, the methods utilizing the Green's potential function are used extensively. For instance, if the Green's function in the Fourier domain is known, the unknown quantity becomes the charge density and the problem of estimating the characteristic parameters is easily solved by using the moment approach [5] or variational techniques [4].

The Green's function is generally calculated for each structure. In this paper, a recurrence algorithm is presented to evaluate the transform of the Green's function for planar open structures having multilayered substrates or superstrates with arbitrary anisotropy. The method is useful, for instance, in calculating the capacitance of planar structures with single or coupled strips in one or more interfaces embedded in multilayered anisotropic dielectrics, including an arbitrary gradient of anisotropy in the normal direction to the interfaces, requiring very little modifications in the programs already existing.

II. Recurrence Formulas for the Potential and Fields in an Anisotropic Layer

Let us first consider a layer of perfect and homogeneous dielectric of finite thickness h. The permittivity tensor at the $x-y$ plane is given by

$$\bar{\bar{\epsilon}} = \begin{pmatrix} \epsilon^{11} & \epsilon^{12} \\ \epsilon^{12} & \epsilon^{22} \end{pmatrix}. \tag{1}$$

Then the bidimensional equation for the electrostatic potential in the Fourier domain has the form

$$\epsilon^{22}\frac{\partial^2\tilde{\phi}}{\partial y^2} + 2j\epsilon^{12}\beta\frac{\partial\tilde{\phi}}{\partial y} - \epsilon^{11}\beta^2\tilde{\phi} = 0. \tag{2}$$

The general solution of this differential equation is

$$\tilde{\phi}(\beta, y) = e^{-j\beta R y}(A\sinh(\beta S y) + B\cosh(\beta S y)) \tag{3}$$

where

$$R = \frac{\epsilon^{12}}{\epsilon^{22}} \tag{4}$$

$$S = \left\{\frac{\epsilon^{11}}{\epsilon^{22}} - \left(\frac{\epsilon^{12}}{\epsilon^{22}}\right)^2\right\}^{1/2}. \tag{5}$$

$\tilde{\phi}(\beta, y)$ is the potential Fourier transform y-coordinate and A and B are arbitrary coefficients which must be determined from the boundary conditions.